

# Modal Decomposition of the von-Kármán Covariance of Atmospheric Turbulence in the Circular Entrance Pupil

Richard J. Mathar\*

*Leiden Observatory, P.O. Box 9513, 2300 RA Leiden, The Netherlands*

(Dated: May 30, 2018)

Estimators of outer scales of atmospheric turbulence usually fit the phase screen snapshots derived from local wave front sensors to a Zernike basis, and then compare the spectrum of expansion coefficients in this basis with a narrowing associated with decreasing outer scales.

This manuscript discusses aspects that arise if the Zernike basis is exchanged for a Karhunen-Loève basis of statistically independent modes. Data acquisition turns out to be more demanding because sensing the tip-tilt mode *is* required. The data reduction methodology is replaced by fitting of variance ratios of an entire (long exposure) data set. Statistical testing of hypotheses on outer scale models can be applied to a set of modes—supposing other noise originating from detector readout and the optical train can be disentangled.

PACS numbers: 95.75.Qr, 95.75.Pq, 42.68.Bz, 42.30.Lr

Keywords: Atmospheric Turbulence, Outer Scale, Karhunen-Loève, von Kármán

## I. STATISTICS OF ATMOSPHERIC TURBULENCE

### A. Measuring and Interpreting Pupil Phases

A contemporary adaptive optics (AO) system of an astronomic telescope measures angles of arrival of the incoming wave front sampled across segmented areas that subdivide the full entrance pupil. The task is to weave the two principal parameters—motion of the image either represented by two Cartesian directions on the detector or by an angle of arrival and azimuth [23]—of the sensor array into a phase function covering the entire pupil. For the purpose of the present work we leave aside aspects of phase unwrapping [19, 29, 33], finite element discretization [34], or noise besides the atmospheric turbulence itself [4].

As the information obtained represents the phase in the pupil, optical path differences integrated along paths through the entire atmosphere and altitudes dependencies are basically not available within a single AO system. Thicknesses and altitude variation of the structure constants may vary [14]. Understanding of the origin of finite outer scales of turbulence remains poor for that reason, and the scattering of outer scale lengths at wavelengths in the visible is significant [2, 13, 15, 38].

Optical path differences from stellar interferometers with baseline lengths of the order of the outer scales promise higher sensitivity. If the interferometric subsystems do not share any data streams with the AO systems of the individual telescopes, the time series of the fringe tracker may be the only information available, and then mediation by some wind velocity with its own set of unknowns is needed to fit the shape of temporal spectra [6, 9, 10] to outer scales. Results from the Palomar Testbed Interferometer merged with tip-tilt information of the telescopes show outer scales of some tens of meters—compatible with data from single-telescope apertures [28].

Auxiliary data products of this kind are not a standard of reduction pipelines of interferometric observations for now, so we discuss only the case of a single circular aperture. The remainder of Section I summarizes the literature on the von Kármán model of outer scales with a single layer with isotropic turbulence. Section II introduces its modal composition for the circular pupil. On the technical side, the matrix elements that arise in the Zernike basis are reduced to Hypergeometric Functions (Section II A), and central obscurations common to on-axis mirror trains are handled in a hybrid form that separates Fourier and real space with the aid of a Neuman series (Section II C). Benefits and problems compared to the use of Zernike covariances are shortly discussed in Section II B.

---

\*URL: <http://www.strw.leidenuniv.nl/~mathar>; Electronic address: mathar@strw.leidenuniv.nl

## B. The von Kármán Model of Outer Scales

The refractive index structure function  $\mathcal{D}_n$  as a function of the 3D separation  $\Delta\mathbf{r}$ , and its Fourier representation  $\Phi_n$  at spatial frequencies  $f$  are related via

$$\mathcal{D}_n(\Delta\mathbf{r}) = 2 \int \Phi_n(f) [1 - \cos(2\pi\mathbf{f} \cdot \Delta\mathbf{r})] d^3f. \quad (1)$$

The von Kármán model of the power spectrum in particular is

$$\Phi_n(f) = c_n C_n^2 (f^2 + f_0^2)^{-(\gamma+3)/2} \quad (2)$$

where  $C_n^2$  is the structure constant which characterizes the global strength of the turbulence, and where  $f_0$  is a wavenumber equal to the inverse of the outer scale.  $\gamma$  is a power spectral index which for our analysis will be set to the Kolmogorov value of 2/3; formulas will generally not be reduced with this value to support independent tests of this scaling [5, 7, 16, 27, 40]. The constant

$$c_n = -\frac{\Gamma(\frac{3+\gamma}{2})}{2\pi^{3/2+\gamma}\Gamma(\frac{-\gamma}{2})} \approx 0.00969315 \quad (\gamma = 2/3) \quad (3)$$

is settled by demanding that at small  $\Delta\mathbf{r}$

$$\mathcal{D}_n(\Delta r) = C_n^2 |\Delta r|^\gamma. \quad (4)$$

This is a model of isotropic turbulence, so the information can be bound to the radial dependencies in real and Fourier space by integration over polar and azimuth angles,

$$\mathcal{D}_n(r) = 8\pi \int_0^\infty f^2 [1 - j_0(2\pi fr)] \Phi_n(f) df = 8\pi c_n C_n^2 \int_0^\infty f^2 [1 - j_0(2\pi fr)] \frac{1}{(f^2 + f_0^2)^{(3+\gamma)/2}} df. \quad (5)$$

Performing the integration leads to a representation in terms of Modified Bessel Functions  $K$  [11, 12, 39],

$$\frac{1}{C_n^2} \mathcal{D}_n(r) r^{-\gamma} = -\frac{(\pi r f_0)^{-\gamma} \Gamma(\gamma/2)}{\Gamma(-\gamma/2)} \left[ 1 - \frac{2}{\Gamma(\gamma/2)} (\pi r f_0)^{\gamma/2} K_{\gamma/2}(2\pi r f_0) \right]. \quad (6)$$

The limit of infinite outer scale recovers the Kolmogorov power law

$$\lim_{f_0 \rightarrow 0} \frac{1}{C_n^2} \mathcal{D}_n(r) r^{-\gamma} = 1, \quad (7)$$

which is the value reached by the curve of  $r = R$  in the left graph of Fig. 1.

## C. Phase Structure Functions

In most applications, the observable is not the three-dimensional distribution of the refractive indices but the phase difference  $\varphi$  between light rays at an optical wavenumber  $\bar{k}$  (which is  $2\pi$  divided by the wavelength). We write  $\mathcal{D}_\varphi$  for the structure function of the phase if observed over a projected distance  $P$  in an input pupil of the instrument after two rays have traveled along parallel lines through a layer of height  $h$  (which includes the air mass factor) in which the refractive index structure function modeled in the previous section defines the statistics. This type of projection onto a two-dimensional plane introduces a weighting of the refractive index power spectrum  $\Phi_n$  with Bessel Functions  $J_0$  [8, 12, 17, 24],

$$\mathcal{D}_\varphi(P) = 4\pi \bar{k}^2 h \int_0^\infty [1 - J_0(2\pi f P)] \Phi_n(f) f df, \quad (8)$$

for the von Kármán spectrum (2) condensed into the well-known

$$\mathcal{D}_\varphi(P) = -\bar{k}^2 h C_n^2 P^{1+\gamma} \frac{\sqrt{\pi}}{\Gamma(-\gamma/2) (\pi P f_0)^{1+\gamma}} \left[ \Gamma\left(\frac{1+\gamma}{2}\right) - 2(\pi P f_0)^{(1+\gamma)/2} K_{(1+\gamma)/2}(2\pi P f_0) \right]. \quad (9)$$

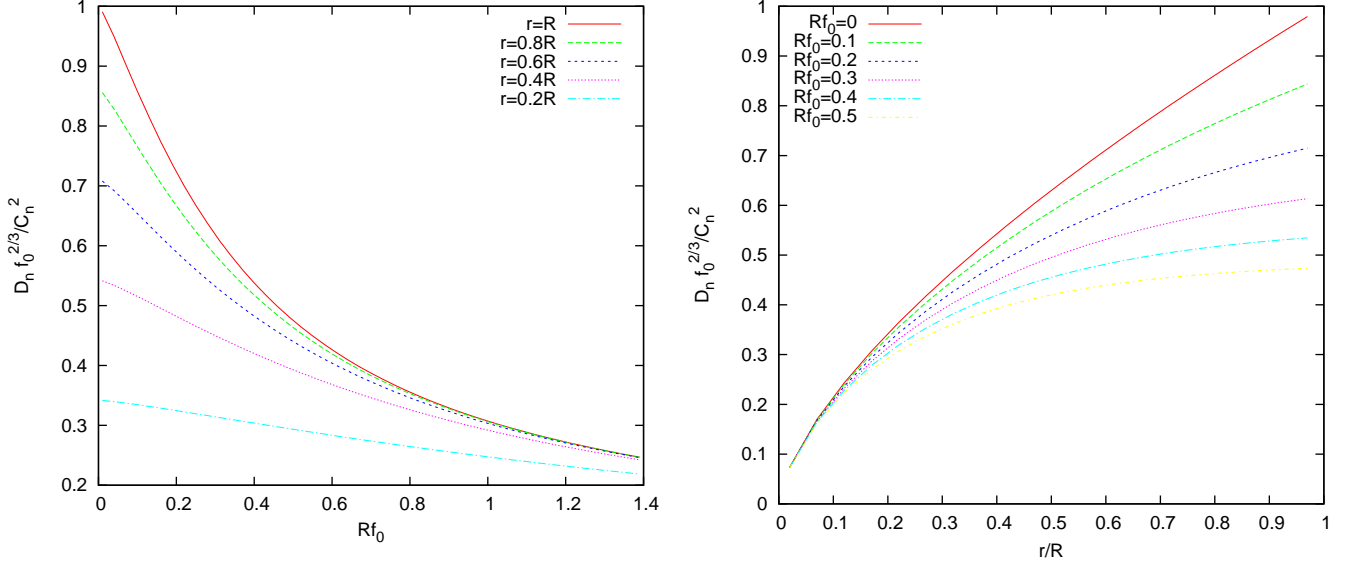


FIG. 1: The refractive index structure function  $\mathcal{D}_n(r)/C_n^2$  of (6) at  $\gamma = 2/3$  as a function of outer scale with the radial distance  $r$  as the parameter, or with the roles of these two dependencies swapped.  $\mathcal{D}_n$  depends essentially on the product  $rf_0$ , so scaling with some anonymous reference length  $R$  leads to the universal curves shown.

The Kolmogorov limit of infinite outer scale is the familiar

$$\lim_{f_0 \rightarrow 0} \mathcal{D}_\varphi(P) = \bar{k}^2 h C_n^2 P^{1+\gamma} g(\gamma) \quad (10)$$

where

$$g(\gamma) \equiv \sqrt{\pi} \frac{\Gamma(-1/2 - \gamma/2)}{\Gamma(-\gamma/2)} \approx 2.9143808, \quad (\gamma = 2/3). \quad (11)$$

Collecting variances of optical path differences from this model—obtained by striking the factor  $\bar{k}^2$  of  $\mathcal{D}_\varphi$ —we notice that the strength of the fluctuations remains smaller than predicted by the factor  $g(\gamma)$  in (11), because this has been derived in the limit  $h/P \rightarrow \infty$  of infinite layer height [24]. For finite  $h/P$ ,

$$\mathcal{D}_\varphi = 2\bar{k}^2 \int_0^h (h - \Delta z) \left[ \mathcal{D}_n(\sqrt{(\Delta z)^2 + P^2}) - \mathcal{D}_n(\Delta z) \right] d(\Delta z) \quad (12)$$

$$= 2\bar{k}^2 C_n^2 P^{\gamma+1} h \int_0^{h/P} \left( 1 - \frac{t}{h/P} \right) \left[ (t^2 + 1)^{\gamma/2} - t^\gamma \right] dt, \quad (13)$$

where the integral can be rephrased as [26, (3.243.1),(3.251.1)]

$$g(\gamma) = 2 \int_0^{h/P} [1 - t/(h/P)] \left[ (1 + t^2)^{\gamma/2} - t^\gamma \right] dt = \frac{h}{P} {}_3F_2 \left( \begin{matrix} -\gamma/2, 1/2, 1 \\ 3/2, 2 \end{matrix} \middle| -\left(\frac{h}{P}\right)^2 \right) - \frac{(h/P)^{1+\gamma}}{(\gamma+1)(1+\gamma/2)}, \quad (14)$$

with [25, 35]

$${}_3F_2 \left( \begin{matrix} -\gamma/2, 1/2, 1 \\ 3/2, 2 \end{matrix} \middle| z \right) = {}_2F_1 \left( \begin{matrix} -\gamma/2, 1/2 \\ 3/2 \end{matrix} \middle| z \right) - {}_2F_1 \left( \begin{matrix} -\gamma/2, 1 \\ 2 \end{matrix} \middle| z \right). \quad (15)$$

This factor cannot reach 2.91 in practise: the layer height  $h$  multiplied by the air mass is limited to the order of 10 km representing the entire atmosphere, and  $P$  is of the order of 2 m for a single telescope up 100 m for an interferometer. Then  $h/P$  is in the range 5000 to 100, and Figure 2 demonstrates that this finite layer thickness places  $g(\gamma)$  in the range 2.2 to 2.6. Long baseline interferometers “miss” some power of  $\mathcal{D}_\varphi$  through this geometric sampling effect.

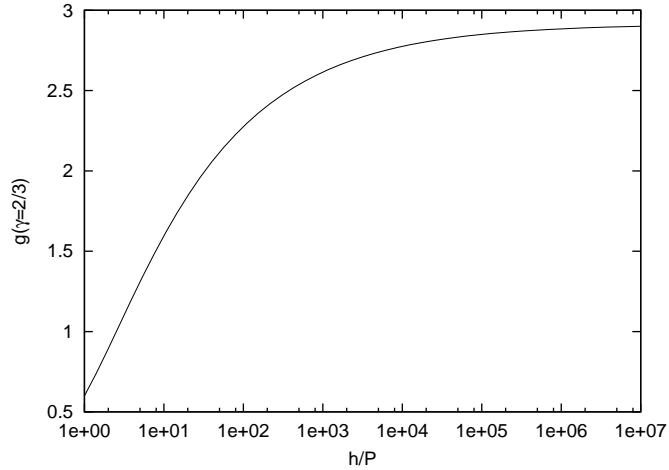


FIG. 2: The undersampling factor (14) as a function of the ratio  $h/P$ .

## II. KARHUNEN-LOÈVE MODES IN THE ENTRANCE PUPIL

### A. Phase Structure Function in the Circular Pupil

Removal of the spatial mean of the structure function (8) defines associated covariances  $C_\varphi$  for two-dimensional vectors  $\mathbf{r}$  in the pupil plane and two-dimensional spatial wavenumbers  $f$ ,

$$C_\varphi(\mathbf{r}) = \int C_\varphi(f) e^{-2\pi i \mathbf{f} \cdot \mathbf{r}} d^2 f = 2\pi \int_0^\infty C_\varphi(f) J_0(2\pi f r) f df, \quad (16)$$

where

$$C_\varphi(f) = \bar{k}^2 h \Phi_n(f). \quad (17)$$

The statistically independent Karhunen-Loève (KL) modes  $F_j$  are eigenvectors of the integral operator [20]

$$\int_{|\mathbf{r}'| < R} C_\varphi(\mathbf{r} - \mathbf{r}') F_j(\mathbf{r}') d^2 r' = \mathcal{B}^2 F_j(\mathbf{r}), \quad (18)$$

where the integration is over the area limited by the pupil radius  $R$ . Moving on to Fourier space, the convolution simplifies to

$$C_\varphi(f) F_j(\mathbf{f}) = \mathcal{B}^2 F_j(\mathbf{f}), \quad (19)$$

and more explicitly with (17) to

$$\bar{k}^2 h c_n C_n^2 \frac{1}{(f^2 + f_0^2)^{(\gamma+3)/2}} F_j(\mathbf{f}) = \mathcal{B}^2 F_j(\mathbf{f}). \quad (20)$$

Introducing dimensionless variables  $\mathbf{r} = R\mathbf{x}$  and  $R\mathbf{f} = \boldsymbol{\sigma}$  helps to gather a set of common constants to unify the analysis,

$$c_n \frac{1}{(\sigma^2 + \sigma_0^2)^{(\gamma+3)/2}} K_p^{(q)}(\boldsymbol{\sigma}) = \frac{\mathcal{B}^2}{\bar{k}^2 h C_n^2 R^{\gamma+3}} K_p^{(q)}(\boldsymbol{\sigma}). \quad (21)$$

The notation assumes that azimuthal dependencies have been split off,

$$K_p^{(q)}(\boldsymbol{\sigma}) = K_p^{(q)}(\sigma) M_q(\theta_\sigma), \quad (22)$$

$$M_q(\theta) = \sqrt{\frac{\varepsilon_q}{2\pi}} \times \begin{cases} \cos(q\theta) \\ \sin(q\theta) \end{cases}; \quad \varepsilon_q \equiv \begin{cases} 1, & q = 0, \\ 1, & |q| \geq 1, \end{cases} \quad (23)$$

such that the two discrete indices  $p$  and  $q$  can be used to enumerate the modes by number of nodes in the radial direction and periodicity along the azimuth  $\theta$ . If the  $K_p^{(q)}(x)$  are expanded in the basis of Zernike polynomials  $R_n^q$ ,

$$\int_0^1 x R_n^q(x) R_{n'}^q(x) dx = \frac{\delta_{n,n'}}{2(n+1)}, \quad (24)$$

$$K_p^{(q)}(x) = \sum_{n \equiv q \pmod{2}} \tau_{n,p,q} \sqrt{2(n+1)} R_n^q(x), \quad (25)$$

Noll's Fourier representation of the  $R_n^q$  induces a Fourier representation of the radial component [32, 36],

$$K_p^{(q)}(\sigma) = \sum_{n \equiv q \pmod{2}} \tau_{n,p,q} \sqrt{2(n+1)} (-1)^{(n-q)/2} i^q \frac{J_{n+1}(2\pi\sigma)}{\sigma} = \sum_{n \equiv q \pmod{2}} \tau_{n,p,q} \sqrt{2(n+1)} i^n \frac{J_{n+1}(2\pi\sigma)}{\sigma} \quad (26)$$

which becomes an eigenvalue equation for the vector of the expansion coefficients  $\tau_{n,p,q}$  [31],

$$c_n (2\pi)^{\gamma+3} \sum_{n \equiv q \pmod{2}} \tau_{n,p,q} \sqrt{2(n+1)} i^{n-n'} \int_0^\infty J_{n+1}(k) J_{n'+1}(k) \frac{dk}{k(k^2+k_0^2)^{(3+\gamma)/2}} = \frac{\mathcal{B}^2}{k^2 h C_n^2 R^{\gamma+3}} \tau_{n',p,q} \frac{1}{\sqrt{2(n'+1)}}. \quad (27)$$

At this stage some arbitrariness remains in scaling both sides of the equation, depending on preferences of normalization to pupil areas, squared diameters or radii. I shall divide through  $g(\gamma)$  to gather  $g(\gamma)$  in front of the  $C_n^2$  of the right hand side to match (10), and shall multiply by a factor

$$2c_\varphi = 2 \left[ 4\Gamma\left(\frac{3+\gamma}{1+\gamma}\right) \right]^{(1+\gamma)/2} = 2 \left[ \frac{24}{5}\Gamma(6/5) \right]^{5/6} \approx 6.883877, \quad (\gamma = 2/3) \quad (28)$$

for compatibility with calculations that introduce a Fried radius as a reference. Altogether,

$$-2c_\varphi \pi \frac{\Gamma(\frac{3}{2} + \frac{\gamma}{2})}{\Gamma(-\frac{1}{2} - \frac{\gamma}{2})} \sum_{n \equiv q \pmod{2}} \tau_{n,p,q} \sqrt{(n+1)(n'+1)} (-1)^{(n-n')/2} I_{nn'} = \lambda_{p,q}^2 \tau_{n',p,q} \quad (29)$$

defining

$$\lambda_{p,q}^2 \equiv \frac{2c_\varphi}{g(\gamma)} \frac{\mathcal{B}^2}{k^2 h C_n^2 (2R)^{\gamma+3}} \quad (30)$$

and

$$I_{nn'} \equiv \int_0^\infty J_{n+1}(k) \frac{1}{k(k^2+k_0^2)^{(3+\gamma)/2}} J_{n'+1}(k) dk. \quad (31)$$

This integral is evaluated as proposed by Winker [38, 41],

$$I_{nn'} = \frac{2}{\pi} \int_0^\infty dk \int_0^{\pi/2} d\theta J_{n+n'+2}(2k \cos \theta) \cos[(n-n')\theta] \frac{1}{k(k^2+k_0^2)^{(3+\gamma)/2}} \quad (32)$$

$$= \frac{2}{\pi} \int_0^\infty dk \int_0^{\pi/2} d\theta \frac{1}{2\pi i} \int_{-i\infty}^{i\infty} ds \frac{\Gamma(-s)(k \cos \theta)^{n+n'+2+2s}}{\Gamma(n+n'+3+s)} \cos[(n-n')\theta] \frac{1}{k(k^2+k_0^2)^{(3+\gamma)/2}} \quad (33)$$

$$\begin{aligned} &= \frac{2}{\pi} \int_0^\infty dk \frac{1}{2\pi i} \int_{-i\infty}^{i\infty} ds \frac{\Gamma(-s) k^{n+n'+2+2s}}{\Gamma(n+n'+3+s)} \frac{\pi \Gamma(n+n'+4+2s)}{2^{n+n'+3+2s} (n+n'+3+2s) \Gamma(n+2+s) \Gamma(n'+2+s)} \frac{1}{k(k^2+k_0^2)^{(3+\gamma)/2}} \\ &= k_0^{n+n'-1-\gamma} \frac{\Gamma(\frac{1+\gamma-n-n'}{2}) \Gamma(\frac{n+n'}{2}+1)}{2^{n+n'+3} \Gamma(n+2) \Gamma(n'+2) \Gamma(\frac{3+\gamma}{2})} \\ &\quad \times {}_3F_4\left(\frac{n+n'}{2}+1, \frac{n+n'}{2}+2, \frac{n+n'+3}{2}; n+2, n'+2, n+n'+3, \frac{1+n+n'-\gamma}{2}; k_0^2\right) \\ &\quad + \frac{\Gamma(\frac{n+n'-1-\gamma}{2}) \Gamma(4+\gamma)}{2^{\gamma+4} \Gamma(\frac{7+\gamma+n+n'}{2}) \Gamma(\frac{5+\gamma+n-n'}{2}) \Gamma(\frac{5+\gamma+n'-n}{2})} \\ &\quad \times {}_3F_4\left(\frac{5+\gamma}{2}, \frac{3+\gamma}{2}, 2+\frac{\gamma}{2}; \frac{5+\gamma+n-n'}{2}, \frac{5+\gamma+n'-n}{2}, \frac{7+\gamma+n+n'}{2}, \frac{3+\gamma-n-n'}{2}; k_0^2\right). \end{aligned} \quad (34)$$

Prototypical results of the calculation are listed in App. A. The reduction of the eigenvalues as the outer scale shrinks is visualized in Fig. 3, and the inward motion of the normalized radial functions  $K_p^{(q)}(x)$  is shown in Fig. 4.

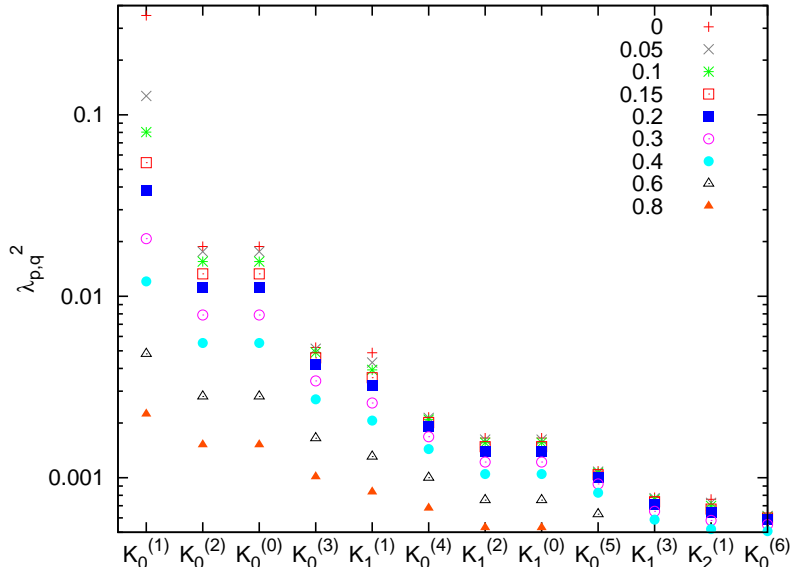


FIG. 3: The eigenvalues  $\lambda_{p,q}^2$  (30) of the KL modes of the phase variance as a function of the outer scale wavenumber  $0 \leq \sigma_0 \leq 0.8$ .

The modes at the largest scales are effected most, as known from earlier analyses [41].

## B. Estimation of Outer Scales

The customary reduction of AO data to outer scales reconstructs the phase as a function of the location in the pupil plane, collects the expansion coefficients of the Zernike expansion, and compares the relative strengths of the coefficients with the reduction predicted as a function of the outer scale [21, 22, 41].

Which new aspects arise if a chart of the KL modes as in Figure 3 is used instead?

Obtaining the expansion coefficients still is a matter of fitting a phase function to a set of modes. One may start with a Zernike basis [30] and convert its coefficients to the KL basis with the aid of Appendix A. The appendix provides the matrix that converts from the Zernike to the KL basis, but no additional computation is demanded because the inverse matrix is the transpose matrix. At this step, the tip-tilt component is an essential ingredient to the process—this is a requirement that was not known to the approach based on the Zernike covariances, and probably disables processing if tip-tilt stages are autonomous and data not available. If a modular approach to information processing of various layers of phase corrections in telescope operation—from course with fringe tracking over medium of tip-tilt stages to fine of adaptive optics—results in a lean system optimized to dispose intermediate data streams irrelevant to the observing astronomer, post-processing of the engineering data concerning components like the atmosphere is put on a diet.

Another modest technical disadvantage is that fitting process becomes iterative in nature because the entries of Appendix A depend on the outer scale, which is the unknown. This is only a matter of producing this static table for a range of outer scales of interest and therefore no real concern.

The conceptual difference is that the data reduction is based on the statistical independence of the KL modes. The outer scale is selected that generates measured variances of the modal coefficients proportional to their  $\lambda_{p,q}^2$ . (The overall factor  $C_n^2$  drops out of the calculation.) The technique does not derive the outer scale from any individual snapshot, but it starts from a hypothetical outer scale, reduces the series of exposures to variances of modal coefficients, and readjusts the value of the outer scale until these variances match that common statistics. In addition, standard statistical methodologies can be applied to derive confidence intervals of the result.

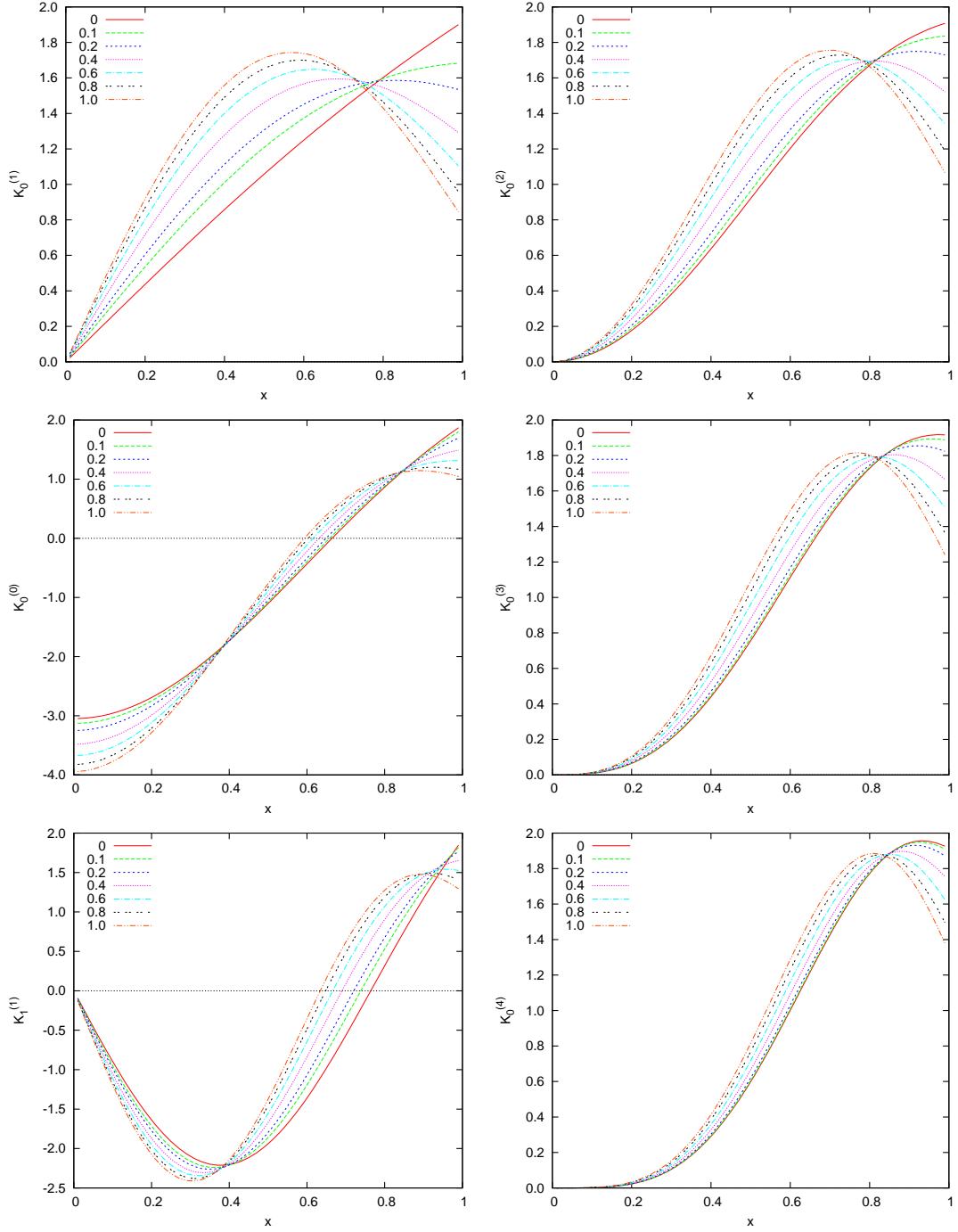


FIG. 4: Influence of the inverse outer scale  $0 \leq \sigma_0 \leq 1$  on some large-scale KL modes (25) of the phase covariance in the circular input pupil.

### C. Central Obscuration

A central obscuration from a secondary mirror removes data up to a radius  $\epsilon$  [measured in units of the pupil radius,  $0 \leq \epsilon \leq 1$ , unrelated to the  $\epsilon$  of (23)] from the areal statistics. The radial component of (22) is represented by the Fourier pair

$$K_p^{(q)}(\sigma) = 2\pi i^q \int_{\epsilon}^1 x dx K_p^{(q)}(x) J_q(2\pi\sigma x), \quad K_p^{(q)}(x) = 2\pi (-i)^q \int_0^{\infty} \sigma d\sigma K_p^{(q)}(\sigma) J_q(2\pi\sigma x), \quad (35)$$

which recovers the results of the previous section if  $\epsilon = 0$ . Insertion of  $K_p^{(q)}(\sigma)$  in (21) yields the eigenvalue equation in mixed coordinates,

$$2\pi(-i)^q c_n \int_0^\infty \frac{1}{(\sigma^2 + \sigma_0^2)^{(\gamma+3)/2}} \sigma K_p^{(q)}(\sigma) J_q(2\pi\sigma x) d\sigma = \frac{\mathcal{B}^2}{k^2 h C_n^2 R^{\gamma+3}} K_p^{(q)}(x). \quad (36)$$

Insertion of (35) and scaling the wave number with  $k \equiv 2\pi\sigma$  means

$$(2\pi)^{\gamma+3} c_n \int_0^\infty dk \frac{1}{(k^2 + k_0^2)^{(\gamma+3)/2}} \int_\epsilon^1 x' dx' K_p^{(q)}(x') k J_q(kx') J_q(kx) = \frac{\mathcal{B}^2}{k^2 h C_n^2 R^{\gamma+3}} K_p^{(q)}(x). \quad (37)$$

The integral over  $k$  is managed by isolating variables [3][18, (§7.15)]

$$\begin{aligned} \frac{k}{2} J_q(kx) J_q(kx') &= (xx')^q \sum_{n \geq 0} (-1)^n (2q + 2n + 1) J_{2q+2n+1}(k) \binom{2q+n}{q} \binom{q+n}{q} \\ &\times {}_2F_1 \left( \begin{matrix} -n, 2q+n+1 \\ q+1 \end{matrix} \mid \sin^2 \phi \right) {}_2F_1 \left( \begin{matrix} -n, 2q+n+1 \\ q+1 \end{matrix} \mid \sin^2 \Phi \right). \end{aligned} \quad (38)$$

Here, the two auxiliary variables  $\phi$  and  $\Phi$  are defined by

$$\cos \phi \cos \Phi = x; \quad \sin \phi \sin \Phi = x', \quad (39)$$

that is

$$\sin^2 \phi = \frac{1 - (x^2 - x'^2) + \sqrt{1 - (x+x')^2} \sqrt{1 - (x-x')^2}}{2}, \quad (40)$$

$$\sin^2 \Phi = \frac{1 - (x^2 - x'^2) - \sqrt{1 - (x+x')^2} \sqrt{1 - (x-x')^2}}{2}. \quad (41)$$

The two Hypergeometric Functions in (38) are Jacobi Polynomials [1, (22.5.42)]. Each term is then integrated with [26, 6.565.8]

$$\begin{aligned} \int_0^\infty \frac{J_{2q+2n+1}(k)}{(k^2 + k_0^2)^{(\gamma+3)/2}} dk &= \frac{k_0^{2q+2n-\gamma-1} \Gamma(1+q+n) \Gamma(\frac{\gamma+1}{2} - q - n)}{4^{q+n+1} \Gamma(\frac{\gamma+3}{2}) \Gamma(2q+2n+2)} {}_1F_2 \left( \begin{matrix} 1+q+n \\ q+n + \frac{1-\gamma}{2}, 2n+2q+2 \end{matrix} \mid \frac{k_0^2}{4} \right) \\ &+ \frac{\Gamma(n+q - \frac{\gamma+1}{2})}{2^{\gamma+3} \Gamma(\frac{\gamma+5}{2} + q+n)} {}_1F_2 \left( \begin{matrix} \frac{\gamma+3}{2} \\ \frac{\gamma+5}{2} + q+n, \frac{\gamma+3}{2} - q-n \end{matrix} \mid \frac{k_0^2}{4} \right). \end{aligned} \quad (42)$$

To avoid that  $x+x' > 1$  in (41), another variable transform  $t = 2k$  is added. The following results have been obtained with a finite element decomposition of the interval  $[\epsilon, 1]$ , and introducing the function

$$\tilde{K}_p^{(q)}(x) \equiv \sqrt{x/2} K_p^{(q)}(x), \quad (43)$$

such that the matrix on the left hand side, which couples each  $x$  to all the  $x'$ , becomes symmetric:

$$(2\pi)^{\gamma+3} \frac{c_n c_\varphi}{g(\gamma)} \int_0^\infty dt \frac{1}{(t^2 + 4k_0^2)^{(\gamma+3)/2}} \int_\epsilon^1 dx' \sqrt{xx'} \tilde{K}_p^{(q)}(x') \frac{t}{2} J_q(tx'/2) J_q(tx/2) = \frac{2c_\varphi}{g(\gamma)} \frac{\mathcal{B}^2}{k^2 h C_n^2 (2R)^{\gamma+3}} \tilde{K}_p^{(q)}(x). \quad (44)$$

The piston mode has been reduced as outlined in Appendix B.

If the radius is selected equivalent to the M2/M1 ratio of the telescopes of the Very Large Telescope, Figure 5 results. Besides the absence of values in the range  $x \leq \epsilon$ , these shapes are hardly different from the full aperture modes of Figure 4.

The variances  $\lambda^2$  in the individual modes are shown in Figure 6. [They are still defined by (30), so comparison of values for different  $\epsilon$  is problematic. One might argue that the reduction of the sampling area and the related decrease in value would warrant a scaling that should depend in one form or the other on  $\epsilon$ . Ultimately, this kind of manipulation is futile, because the  $\lambda^2$  do not depend only on the pupil area but also on its shape.] A noticeable effect is the break-up of the degeneracy of the values for  $K_p^{(2)}$  and  $K_p^{(0)}$  as  $\epsilon$  increases. It is plausible that modes that do not have a node in the middle of the pupil are more sensitive to blanking of the center part than modes that approach zero as  $x \rightarrow 0$ .



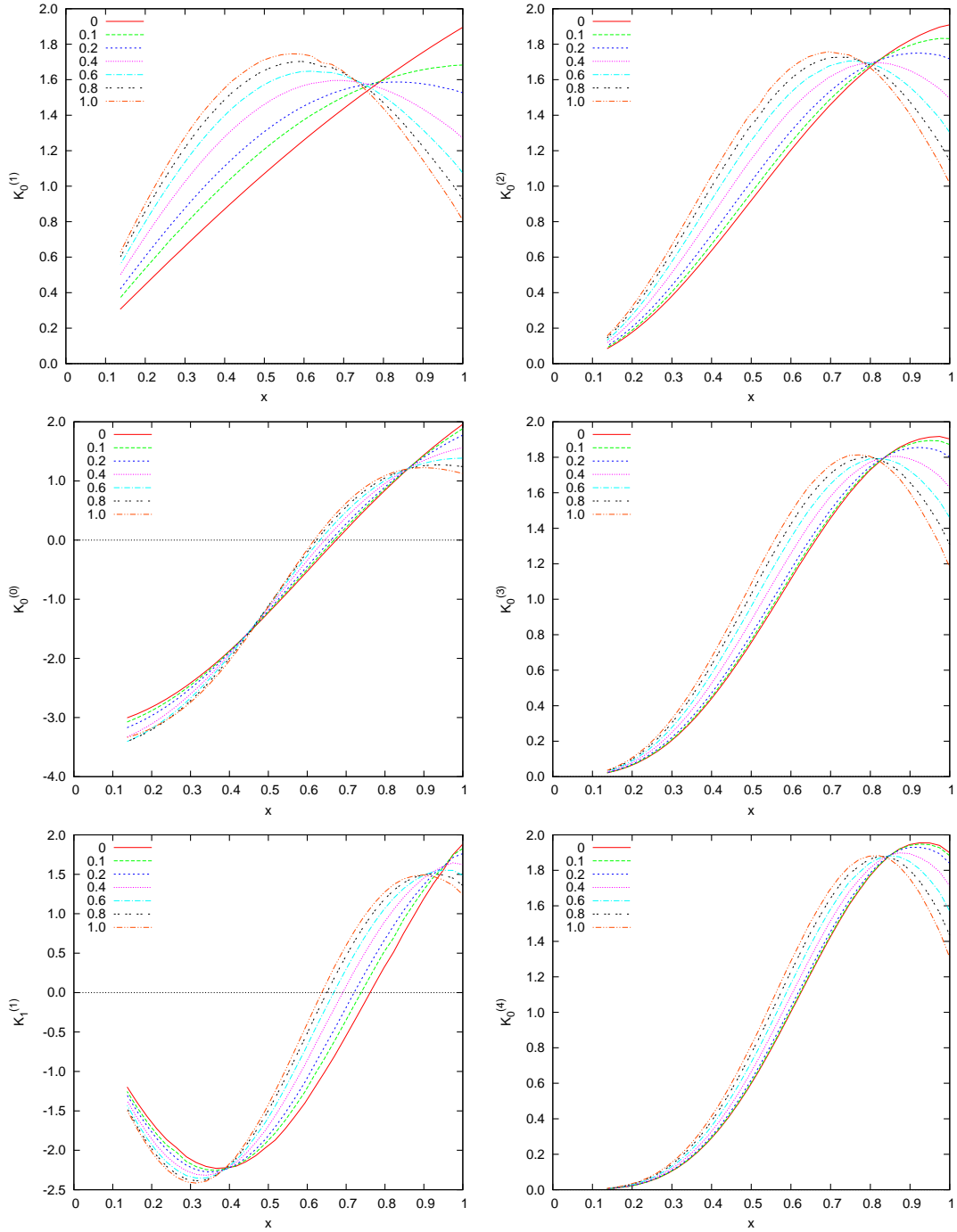


FIG. 5: Large-scale KL modes  $K_p^{(q)}(x)$  with a central obscuration of radius  $\epsilon = 0.1369$  for a set of inverse outer scales from 0 to 1.0.

### III. SUMMARY

The text demonstrates computation of the statistically independent modes of phase screens in the von Kármán class of outer scales sampled over spherical receiver pupils, optionally taking into account masking of a circular region in the center. The main value in this work resides in techniques to compute integrals in the eigenvalue problem.

These modes can be employed to compute outer scales from measured phase functions. The goodness-of-fit of the von Kármán modal spectrum can be addressed. The number of degrees of freedom depends on how many of the modes remain free from other genuine sources of noise besides atmospheric turbulence.

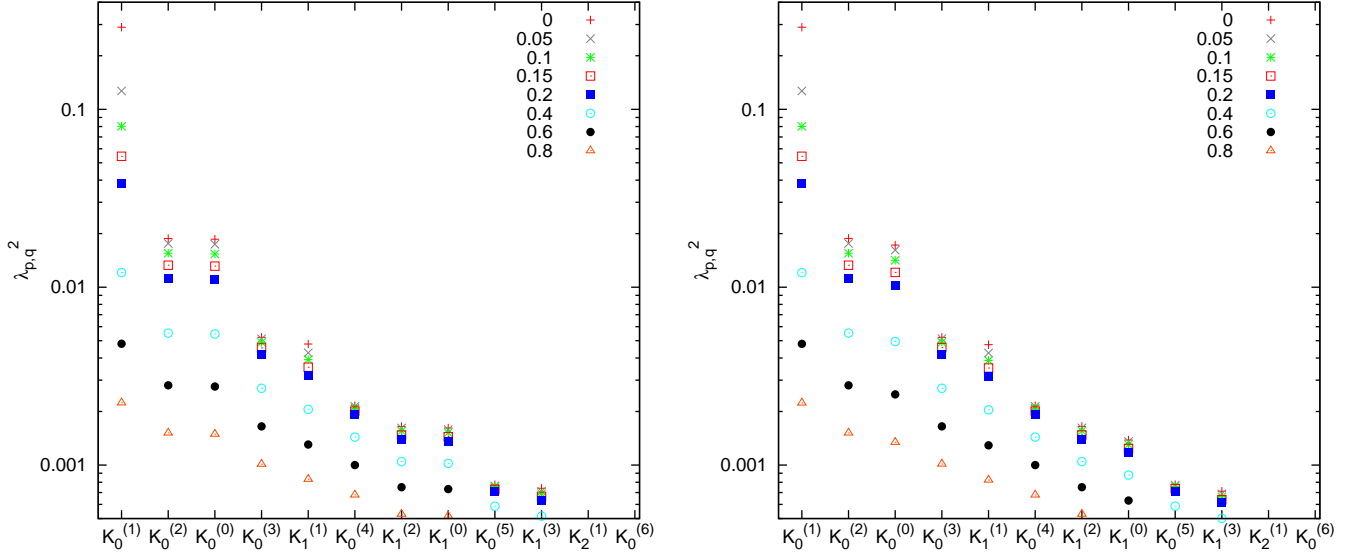


FIG. 6: Modal eigenvalues for  $\epsilon = 0.0462$  (left, roughly representative of the Keck center tile size) and  $\epsilon = 0.1369$  (right) with different symbols for inverse outer scales  $\sigma_0$  from 0 to 0.8.

### Appendix A: Karhunen-Loève Modes of the Phase Covariance Inside the Circular Pupil

Explicit expansions of the first (large-scale) modes (22) follow for dimensionless inverse outer scales from 0.05 to 1. The case of infinite outer scale,  $\sigma_0 = 0$ , has been published before [31] and is not duplicated here. Each line shows the eigenvalue (30), a colon, the azimuthal parameter  $|q|$ , another colon, and a sum over Zernike functions using Noll's indexing [32]. The  $\sin(q\theta)$  and  $\cos(q\theta)$  are basically degenerate if  $q \neq 0$ : two modes share the same radial  $K_p^{(q)}(x)$  and  $\lambda_{p,q}^2$  and differ only in  $M_q(\theta)$ . A notation with two comma-separated indices for  $Z$  condenses them into a single line, and choosing either the left or the right number in the index pairs selects a unique  $K_p^{(q)}(\mathbf{x})$ .

The squared coefficients sum up to  $1/\pi$  to cancel Noll's normalization of the Zernike basis and to end up with a  $K_p^{(q)}$  normalized to unity.

$\sigma_0 = 0.05$ :

```

0.1270639 : 1: +0.5621830*Z(2,3) -0.0474462*Z(8,7) +0.0030025*Z(16,17) -0.0000182*Z(30,29)
+0.0000032*Z(46,47)

0.0176247 : 2: +0.5540843*Z(6,5) -0.1056709*Z(12,13) +0.0115730*Z(24,23) -0.0004187*Z(38,39)
+0.0000243*Z(58,57) +0.0000014*Z(80,81)

0.0176247 : 0: +0.5540843*Z(1) -0.1056709*Z(4) +0.0115730*Z(11) -0.0004187*Z(22) +0.0000243*Z(37)
+0.0000014*Z(56)

0.0051337 : 3: +0.5411529*Z(10,9) -0.1576676*Z(18,19) +0.0245247*Z(32,31) -0.0016922*Z(48,49)
+0.0001077*Z(70,69)

0.0043151 : 1: +0.0457305*Z(2,3) +0.5301453*Z(8,7) -0.1848336*Z(16,17) +0.0315406*Z(30,29)
-0.0025078*Z(46,47) +0.0001649*Z(68,67) -0.0000020*Z(92,93) +0.0000011*Z(122,121)

0.0021374 : 4: +0.5271594*Z(14,15) -0.1971752*Z(26,25) +0.0389824*Z(40,41) -0.0038784*Z(60,59)
+0.0003054*Z(82,83) -0.0000094*Z(110,109) +0.0000018*Z(140,141)

0.0016213 : 2: +0.0990281*Z(6,5) +0.4914390*Z(12,13) -0.2517952*Z(24,23) +0.0594666*Z(38,39)
-0.0073175*Z(58,57) +0.0006477*Z(80,81) -0.0000312*Z(108,107) +0.0000032*Z(138,139)

0.0016213 : 0: +0.0990281*Z(1) +0.4914390*Z(4) -0.2517952*Z(11) +0.0594666*Z(22) -0.0073175*Z(37)
+0.0006477*Z(56) -0.0000312*Z(79) +0.0000032*Z(106)

```

0.0010797 : 5: +0.5135000\*Z(20,21) -0.2273859\*Z(34,33) +0.0536290\*Z(50,51) -0.0068392\*Z(72,71)  
+0.0006548\*Z(96,97) -0.0000348\*Z(126,125) +0.0000037\*Z(158,159)

0.0007713 : 3: +0.1435201\*Z(10,9) +0.4445464\*Z(18,19) -0.3025397\*Z(32,31) +0.0912672\*Z(48,49)  
-0.0150800\*Z(70,69) +0.0017271\*Z(94,95) -0.0001286\*Z(124,123) +0.0000102\*Z(156,157)

$\sigma_0 = 0.1:$

0.0802920 : 1: +0.5603194\*Z(2,3) -0.0658073\*Z(8,7) +0.0046317\*Z(16,17) -0.0000506\*Z(30,29)  
+0.0000052\*Z(46,47)

0.0155178 : 2: +0.5522704\*Z(6,5) -0.1146220\*Z(12,13) +0.0129920\*Z(24,23) -0.0005054\*Z(38,39)  
+0.0000290\*Z(58,57) +0.0000014\*Z(80,81)

0.0155178 : 0: +0.5522704\*Z(1) -0.1146220\*Z(4) +0.0129920\*Z(11) -0.0005054\*Z(22) +0.0000290\*Z(37)  
+0.0000014\*Z(56)

0.0049007 : 3: +0.5400346\*Z(10,9) -0.1613201\*Z(18,19) +0.0254004\*Z(32,31) -0.0017817\*Z(48,49)  
+0.0001143\*Z(70,69)

0.0039238 : 1: +0.0631227\*Z(2,3) +0.5235370\*Z(8,7) -0.1974575\*Z(16,17) +0.0351595\*Z(30,29)  
-0.0029586\*Z(46,47) +0.0001991\*Z(68,67) -0.0000034\*Z(92,93) +0.0000013\*Z(122,121)

0.0020876 : 4: +0.5264522\*Z(14,15) -0.1989426\*Z(26,25) +0.0395483\*Z(40,41) -0.0039580\*Z(60,59)  
+0.0003132\*Z(82,83) -0.0000098\*Z(110,109) +0.0000019\*Z(140,141)

0.0015585 : 2: +0.1070746\*Z(6,5) +0.4864405\*Z(12,13) -0.2575283\*Z(24,23) +0.0619577\*Z(38,39)  
-0.0077766\*Z(58,57) +0.0006978\*Z(80,81) -0.0000347\*Z(108,107) +0.0000034\*Z(138,139)

0.0015585 : 0: +0.1070746\*Z(1) +0.4864405\*Z(4) -0.2575283\*Z(11) +0.0619577\*Z(22) -0.0077766\*Z(37)  
+0.0006978\*Z(56) -0.0000347\*Z(79) +0.0000034\*Z(106)

0.0010641 : 5: +0.5130108\*Z(20,21) -0.2283914\*Z(34,33) +0.0540274\*Z(50,51) -0.0069096\*Z(72,71)  
+0.0006633\*Z(96,97) -0.0000353\*Z(126,125) +0.0000038\*Z(158,159)

0.0007576 : 3: +0.1466064\*Z(10,9) +0.4417699\*Z(18,19) -0.3046954\*Z(32,31) +0.0926064\*Z(48,49)  
-0.0154085\*Z(70,69) +0.0017748\*Z(94,95) -0.0001332\*Z(124,123) +0.0000106\*Z(156,157)

$\sigma_0 = 0.15:$

0.0544954 : 1: +0.5580974\*Z(2,3) -0.0824405\*Z(8,7) +0.0063821\*Z(16,17) -0.0000923\*Z(30,29)  
+0.0000081\*Z(46,47)

0.0132897 : 2: +0.5500307\*Z(6,5) -0.1247356\*Z(12,13) +0.0147219\*Z(24,23) -0.0006141\*Z(38,39)  
+0.0000353\*Z(58,57) +0.0000015\*Z(80,81)

0.0132897 : 0: +0.5500307\*Z(1) -0.1247356\*Z(4) +0.0147219\*Z(11) -0.0006141\*Z(22) +0.0000353\*Z(37)  
+0.0000015\*Z(56)

0.0045724 : 3: +0.5384109\*Z(10,9) -0.1664591\*Z(18,19) +0.0266702\*Z(32,31) -0.0019125\*Z(48,49)  
+0.0001243\*Z(70,69) +0.0000010\*Z(124,123)

0.0035533 : 1: +0.0787021\*Z(2,3) +0.5165478\*Z(8,7) -0.2092330\*Z(16,17) +0.0387812\*Z(30,29)  
-0.0034279\*Z(46,47) +0.0002365\*Z(68,67) -0.0000049\*Z(92,93) +0.0000014\*Z(122,121)

0.0020105 : 4: +0.5253405\*Z(14,15) -0.2016812\*Z(26,25) +0.0404365\*Z(40,41) -0.0040835\*Z(60,59)  
+0.0003256\*Z(82,83) -0.0000104\*Z(110,109) +0.0000019\*Z(140,141)

0.0014813 : 2: +0.1160947\*Z(6,5) +0.4804411\*Z(12,13) -0.2640555\*Z(24,23) +0.0649074\*Z(38,39)  
-0.0083296\*Z(58,57) +0.0007596\*Z(80,81) -0.0000389\*Z(108,107) +0.0000037\*Z(138,139)

0.0014813 : 0: +0.1160947\*Z(1) +0.4804411\*Z(4) -0.2640555\*Z(11) +0.0649074\*Z(22) -0.0083296\*Z(37)  
+0.0007596\*Z(56) -0.0000389\*Z(79) +0.0000037\*Z(106)

0.0010391 : 5: +0.5122189\*Z(20,21) -0.2300063\*Z(34,33) +0.0546713\*Z(50,51) -0.0070238\*Z(72,71)  
+0.0006773\*Z(96,97) -0.0000363\*Z(126,125) +0.0000039\*Z(158,159)

0.0007373 : 3: +0.1509283\*Z(10,9) +0.4377755\*Z(18,19) -0.3077212\*Z(32,31) +0.0945258\*Z(48,49)  
-0.0158828\*Z(70,69) +0.0018443\*Z(94,95) -0.0001398\*Z(124,123) +0.0000111\*Z(156,157)

$\sigma_0 = 0.2:$

0.0384868 : 1: +0.5555830\*Z(2,3) -0.0978254\*Z(8,7) +0.0082237\*Z(16,17) -0.0001412\*Z(30,29)  
+0.0000118\*Z(46,47) +0.0000011\*Z(68,67)

0.0112251 : 2: +0.5475076\*Z(6,5) -0.1351598\*Z(12,13) +0.0166326\*Z(24,23) -0.0007383\*Z(38,39)  
+0.0000432\*Z(58,57) +0.0000017\*Z(80,81)

0.0112251 : 0: +0.5475076\*Z(1) -0.1351598\*Z(4) +0.0166326\*Z(11) -0.0007383\*Z(22) +0.0000432\*Z(37)  
+0.0000017\*Z(56)

0.0041940 : 3: +0.5364214\*Z(10,9) -0.1725149\*Z(18,19) +0.0282171\*Z(32,31) -0.0020739\*Z(48,49)  
+0.0001371\*Z(70,69) +0.0000011\*Z(124,123)

0.0032042 : 1: +0.0929350\*Z(2,3) +0.5092242\*Z(8,7) -0.2203375\*Z(16,17) +0.0424228\*Z(30,29)  
-0.0039175\*Z(46,47) +0.0002775\*Z(68,67) -0.0000066\*Z(92,93) +0.0000016\*Z(122,121)

0.0019126 : 4: +0.5238905\*Z(14,15) -0.2051844\*Z(26,25) +0.0415913\*Z(40,41) -0.0042476\*Z(60,59)  
+0.0003420\*Z(82,83) -0.0000111\*Z(110,109) +0.0000020\*Z(140,141)

0.0013966 : 2: +0.1252979\*Z(6,5) +0.4738551\*Z(12,13) -0.2708383\*Z(24,23) +0.0681004\*Z(38,39)  
-0.0089399\*Z(58,57) +0.0008295\*Z(80,81) -0.0000438\*Z(108,107) +0.0000041\*Z(138,139)

0.0013966 : 0: +0.1252979\*Z(1) +0.4738551\*Z(4) -0.2708383\*Z(11) +0.0681004\*Z(22) -0.0089399\*Z(37)  
+0.0008295\*Z(56) -0.0000438\*Z(79) +0.0000041\*Z(106)

0.0010062 : 5: +0.5111531\*Z(20,21) -0.2321555\*Z(34,33) +0.0555358\*Z(50,51) -0.0071778\*Z(72,71)  
+0.0006962\*Z(96,97) -0.0000375\*Z(126,125) +0.0000040\*Z(158,159)

0.0007122 : 3: +0.1559847\*Z(10,9) +0.4329305\*Z(18,19) -0.3112822\*Z(32,31) +0.0968427\*Z(48,49)  
-0.0164612\*Z(70,69) +0.0019301\*Z(94,95) -0.0001480\*Z(124,123) +0.0000118\*Z(156,157)

$\sigma_0 = 0.3:$

0.0207627 : 1: +0.5499437\*Z(2,3) -0.1254079\*Z(8,7) +0.0120252\*Z(16,17) -0.0002530\*Z(30,29)  
+0.0000226\*Z(46,47) +0.0000019\*Z(68,67)

0.0078797 : 2: +0.5419000\*Z(6,5) -0.1556381\*Z(12,13) +0.0207357\*Z(24,23) -0.0010191\*Z(38,39)  
+0.0000634\*Z(58,57) +0.0000021\*Z(80,81)

0.0078797 : 0: +0.5419000\*Z(1) -0.1556381\*Z(4) +0.0207357\*Z(11) -0.0010191\*Z(22) +0.0000634\*Z(37)  
+0.0000021\*Z(56)

0.0034105 : 3: +0.5317006\*Z(10,9) -0.1859701\*Z(18,19) +0.0318335\*Z(32,31) -0.0024607\*Z(48,49)  
+0.0001696\*Z(70,69) -0.0000011\*Z(94,95) +0.0000013\*Z(124,123)

0.0025805 : 1: +0.1179237\*Z(2,3) +0.4939434\*Z(8,7) -0.2406863\*Z(16,17) +0.0496921\*Z(30,29)  
-0.0049451\*Z(46,47) +0.0003693\*Z(68,67) -0.0000106\*Z(92,93) +0.0000020\*Z(122,121)

0.0016809 : 4: +0.5202115\*Z(14,15) -0.2137474\*Z(26,25) +0.0444970\*Z(40,41) -0.0046666\*Z(60,59)  
+0.0003854\*Z(82,83) -0.0000130\*Z(110,109) +0.0000023\*Z(140,141)

0.0012199 : 2: +0.1430463\*Z(6,5) +0.4596855\*Z(12,13) -0.2843055\*Z(24,23) +0.0748388\*Z(38,39)  
-0.0102679\*Z(58,57) +0.0009874\*Z(80,81) -0.0000551\*Z(108,107) +0.0000049\*Z(138,139)

0.0012199 : 0: +0.1430463\*Z(1) +0.4596855\*Z(4) -0.2843055\*Z(11) +0.0748388\*Z(22) -0.0102679\*Z(37)

+0.0009874\*Z(56) -0.0000551\*Z(79) +0.0000049\*Z(106)

0.0009225 : 5: +0.5083277\*Z(20,21) -0.2377231\*Z(34,33) +0.0578144\*Z(50,51) -0.0075872\*Z(72,71)  
+0.0007473\*Z(96,97) -0.0000409\*Z(126,125) +0.0000043\*Z(158,159)

0.0006527 : 3: +0.1670529\*Z(10,9) +0.4216099\*Z(18,19) -0.3191848\*Z(32,31) +0.1022108\*Z(48,49)  
-0.0178264\*Z(70,69) +0.0021369\*Z(94,95) -0.0001680\*Z(124,123) +0.0000134\*Z(156,157)

$\sigma_0 = 0.4:$

0.0120802 : 1: +0.5438669\*Z(2,3) -0.1492296\*Z(8,7) +0.0157816\*Z(16,17) -0.0003729\*Z(30,29)  
+0.0000384\*Z(46,47) +0.0000031\*Z(68,67)

0.0055228 : 2: +0.5358544\*Z(6,5) -0.1747716\*Z(12,13) +0.0249608\*Z(24,23) -0.0013265\*Z(38,39)  
+0.0000892\*Z(58,57) +0.0000027\*Z(80,81) +0.0000011\*Z(108,107)

0.0055228 : 0: +0.5358544\*Z(1) -0.1747716\*Z(4) +0.0249608\*Z(11) -0.0013265\*Z(22) +0.0000892\*Z(37)  
+0.0000027\*Z(56) +0.0000011\*Z(79)

0.0027015 : 3: +0.5263645\*Z(10,9) -0.1998967\*Z(18,19) +0.0358207\*Z(32,31) -0.0029028\*Z(48,49)  
+0.0002098\*Z(70,69) -0.0000017\*Z(94,95) +0.0000016\*Z(124,123)

0.0020613 : 1: +0.1388056\*Z(2,3) +0.4783720\*Z(8,7) -0.2587251\*Z(16,17) +0.0568160\*Z(30,29)  
-0.0060141\*Z(46,47) +0.0004724\*Z(68,67) -0.0000151\*Z(92,93) +0.0000025\*Z(122,121)

0.0014359 : 4: +0.5158045\*Z(14,15) -0.2234543\*Z(26,25) +0.0479255\*Z(40,41) -0.0051719\*Z(60,59)  
+0.0004400\*Z(82,83) -0.0000153\*Z(110,109) +0.0000027\*Z(140,141)

0.0010481 : 2: +0.1591466\*Z(6,5) +0.4448988\*Z(12,13) -0.2970362\*Z(24,23) +0.0817255\*Z(38,39)  
-0.0116808\*Z(58,57) +0.0011637\*Z(80,81) -0.0000680\*Z(108,107) +0.0000059\*Z(138,139)

0.0010481 : 0: +0.1591466\*Z(1) +0.4448988\*Z(4) -0.2970362\*Z(11) +0.0817255\*Z(22) -0.0116808\*Z(37)  
+0.0011637\*Z(56) -0.0000680\*Z(79) +0.0000059\*Z(106)

0.0008254 : 5: +0.5047821\*Z(20,21) -0.2444603\*Z(34,33) +0.0606444\*Z(50,51) -0.0081031\*Z(72,71)  
+0.0008134\*Z(96,97) -0.0000452\*Z(126,125) +0.0000048\*Z(158,159)

0.0005874 : 3: +0.1782251\*Z(10,9) +0.4090493\*Z(18,19) -0.3273494\*Z(32,31) +0.1081019\*Z(48,49)  
-0.0193653\*Z(70,69) +0.0023770\*Z(94,95) -0.0001917\*Z(124,123) +0.0000154\*Z(156,157)

$\sigma_0 = 0.6:$

0.0048075 : 1: +0.5316377\*Z(2,3) -0.1875067\*Z(8,7) +0.0226296\*Z(16,17) -0.0006127\*Z(30,29)  
+0.0000863\*Z(46,47) +0.0000078\*Z(68,67) +0.0000016\*Z(92,93)

0.0028053 : 2: +0.5234235\*Z(6,5) -0.2079357\*Z(12,13) +0.0331139\*Z(24,23) -0.0019680\*Z(38,39)  
+0.0001565\*Z(58,57) +0.0000053\*Z(80,81) +0.0000020\*Z(108,107)

0.0028053 : 0: +0.5234235\*Z(1) -0.2079357\*Z(4) +0.0331139\*Z(11) -0.0019680\*Z(22) +0.0001565\*Z(37)  
+0.0000053\*Z(56) +0.0000020\*Z(79)

0.0016497 : 3: +0.5149116\*Z(10,9) -0.2263237\*Z(18,19) +0.0440286\*Z(32,31) -0.0038640\*Z(48,49)  
+0.0003090\*Z(70,69) -0.0000025\*Z(94,95) +0.0000025\*Z(124,123)

0.0013057 : 1: +0.1704452\*Z(2,3) +0.4481773\*Z(8,7) -0.2887852\*Z(16,17) +0.0702216\*Z(30,29)  
-0.0081810\*Z(46,47) +0.0007039\*Z(68,67) -0.0000250\*Z(92,93) +0.0000039\*Z(122,121)

0.0009994 : 4: +0.5058217\*Z(14,15) -0.2435913\*Z(26,25) +0.0554728\*Z(40,41) -0.0063270\*Z(60,59)  
+0.0005743\*Z(82,83) -0.0000206\*Z(110,109) +0.0000037\*Z(140,141)

0.0007519 : 2: +0.1855962\*Z(6,5) +0.4154116\*Z(12,13) -0.3194096\*Z(24,23) +0.0951789\*Z(38,39)  
-0.0146004\*Z(58,57) +0.0015527\*Z(80,81) -0.0000970\*Z(108,107) +0.0000085\*Z(138,139)

0.0007519 : 0: +0.1855962\*Z(1) +0.4154116\*Z(4) -0.3194096\*Z(11) +0.0951789\*Z(22) -0.0146004\*Z(37)  
+0.0015527\*Z(56) -0.0000970\*Z(79) +0.0000085\*Z(106)

0.0006290 : 5: +0.4963318\*Z(20,21) -0.2595260\*Z(34,33) +0.0672512\*Z(50,51) -0.0093399\*Z(72,71)  
+0.0009791\*Z(96,97) -0.0000558\*Z(126,125) +0.0000061\*Z(158,159)

0.0004592 : 3: +0.1984313\*Z(10,9) +0.3826865\*Z(18,19) -0.3427694\*Z(32,31) +0.1202986\*Z(48,49)  
-0.0226871\*Z(70,69) +0.0029188\*Z(94,95) -0.0002463\*Z(124,123) +0.0000203\*Z(156,157)

$\sigma_0 = 0.8$ :

0.0022407 : 1: +0.5203650\*Z(2,3) -0.2161624\*Z(8,7) +0.0283406\*Z(16,17) -0.0008481\*Z(30,29)  
+0.0001528\*Z(46,47) +0.0000171\*Z(68,67) +0.0000034\*Z(92,93)

0.0015169 : 2: +0.5114918\*Z(6,5) -0.2346225\*Z(12,13) +0.0403918\*Z(24,23) -0.0025985\*Z(38,39)  
+0.0002410\*Z(58,57) +0.0000108\*Z(80,81) +0.0000035\*Z(108,107)

0.0015169 : 0: +0.5114918\*Z(1) -0.2346225\*Z(4) +0.0403918\*Z(11) -0.0025985\*Z(22) +0.0002410\*Z(37)  
+0.0000108\*Z(56) +0.0000035\*Z(79)

0.0010125 : 3: +0.5034249\*Z(10,9) -0.2493257\*Z(18,19) +0.0518292\*Z(32,31) -0.0048426\*Z(48,49)  
+0.0004262\*Z(70,69) -0.0000017\*Z(94,95) +0.0000039\*Z(124,123)

0.0008339 : 1: +0.1919391\*Z(2,3) +0.4207723\*Z(8,7) -0.3123424\*Z(16,17) +0.0821921\*Z(30,29)  
-0.0102809\*Z(46,47) +0.0009559\*Z(68,67) -0.0000348\*Z(92,93) +0.0000058\*Z(122,121)  
+0.0000011\*Z(154,155)

0.0006790 : 4: +0.4953154\*Z(14,15) -0.2625515\*Z(26,25) +0.0631000\*Z(40,41) -0.0075552\*Z(60,59)  
+0.0007312\*Z(82,83) -0.0000257\*Z(110,109) +0.0000052\*Z(140,141) +0.0000010\*Z(176,175)

0.0005307 : 2: +0.2050703\*Z(6,5) +0.3877207\*Z(12,13) -0.3376902\*Z(24,23) +0.1076308\*Z(38,39)  
-0.0174870\*Z(58,57) +0.0019688\*Z(80,81) -0.0001283\*Z(108,107) +0.0000118\*Z(138,139)

0.0005307 : 0: +0.2050703\*Z(1) +0.3877207\*Z(4) -0.3376902\*Z(11) +0.1076308\*Z(22) -0.0174870\*Z(37)  
+0.0019688\*Z(56) -0.0001283\*Z(79) +0.0000118\*Z(106)

0.0004624 : 5: +0.4870068\*Z(20,21) -0.2747635\*Z(34,33) +0.0743178\*Z(50,51) -0.0107141\*Z(72,71)  
+0.0011749\*Z(96,97) -0.0000677\*Z(126,125) +0.0000079\*Z(158,159)

0.0003491 : 3: +0.2146554\*Z(10,9) +0.3567923\*Z(18,19) -0.3560623\*Z(32,31) +0.1321324\*Z(48,49)  
-0.0260852\*Z(70,69) +0.0035049\*Z(94,95) -0.0003067\*Z(124,123) +0.0000262\*Z(156,157)

$\sigma_0 = 1.0$ :

0.0011717 : 1: +0.5104798\*Z(2,3) -0.2379706\*Z(8,7) +0.0329996\*Z(16,17) -0.0010862\*Z(30,29)  
+0.0002291\*Z(46,47) +0.0000318\*Z(68,67) +0.0000066\*Z(92,93) +0.0000016\*Z(122,121)

0.0008736 : 2: +0.5006014\*Z(6,5) -0.2559705\*Z(12,13) +0.0466574\*Z(24,23) -0.0031965\*Z(38,39)  
+0.0003360\*Z(58,57) +0.0000203\*Z(80,81) +0.0000060\*Z(108,107) +0.0000015\*Z(138,139)

0.0008736 : 0: +0.5006014\*Z(1) -0.2559705\*Z(4) +0.0466574\*Z(11) -0.0031965\*Z(22) +0.0003360\*Z(37)  
+0.0000203\*Z(56) +0.0000060\*Z(79) +0.0000015\*Z(106)

0.0006374 : 3: +0.4925470\*Z(10,9) -0.2687151\*Z(18,19) +0.0588705\*Z(32,31) -0.0057865\*Z(48,49)  
+0.0005542\*Z(70,69) +0.0000017\*Z(94,95) +0.0000061\*Z(124,123) +0.0000015\*Z(156,157)

0.0005433 : 1: +0.2065358\*Z(2,3) +0.3967198\*Z(8,7) -0.3309519\*Z(16,17) +0.0926588\*Z(30,29)  
-0.0122456\*Z(46,47) +0.0012152\*Z(68,67) -0.0000426\*Z(92,93) +0.0000086\*Z(122,121)  
+0.0000016\*Z(154,155)

0.0004619 : 4: +0.4849996\*Z(14,15) -0.2794018\*Z(26,25) +0.0703001\*Z(40,41) -0.0087740\*Z(60,59)  
+0.0009009\*Z(82,83) -0.0000295\*Z(110,109) +0.0000073\*Z(140,141) +0.0000014\*Z(176,175)

$$0.0003744 : 2: +0.2190750*Z(6,5) +0.3626864*Z(12,13) -0.3524757*Z(24,23) +0.1188288*Z(38,39) \\ -0.0202349*Z(58,57) +0.0023925*Z(80,81) -0.0001595*Z(108,107) +0.0000158*Z(138,139) \\ +0.0000012*Z(174,173)$$

$$0.0003744 : 0: +0.2190750*Z(1) +0.3626864*Z(4) -0.3524757*Z(11) +0.1188288*Z(22) -0.0202349*Z(37) \\ +0.0023925*Z(56) -0.0001595*Z(79) +0.0000158*Z(106) +0.0000012*Z(137)$$

$$0.0003356 : 5: +0.4775241*Z(20,21) -0.2890089*Z(34,33) +0.0812749*Z(50,51) -0.0121207*Z(72,71) \\ +0.0013880*Z(96,97) -0.0000795*Z(126,125) +0.0000103*Z(158,159) +0.0000013*Z(196,195)$$

$$0.0002623 : 3: -0.2270448*Z(10,9) -0.3325947*Z(18,19) +0.3671201*Z(32,31) -0.1431189*Z(48,49) \\ +0.0293962*Z(70,69) -0.0041058*Z(94,95) +0.0003695*Z(124,123) -0.0000330*Z(156,157)$$

## Appendix B: Piston Removal

The piston mode over the annulus is a mode without azimuth dependence,  $q = 0$ , where  $K_p^{(0)}(x)$  is a constant that does not depend on the radial coordinate  $x$ . Finite outer scales,  $k_0 > 0$ , prohibit the ultraviolet divergence of the integrals that is characteristic to the Kolmogorov variance, so piston subtraction could be implemented by ignoring the associated mode. Yet, removal of the piston improves numerical stability because this contribution otherwise dominates the matrix elements at  $q = 0$ .

At  $q = 0$ , equation (38) reads

$$\frac{k}{2} J_0(kx) J_0(kx') = \sum_{n \geq 0} (-1)^n (2n+1) J_{2n+1}(k) \\ \times {}_2F_1 \left( \begin{matrix} -n, n+1 \\ 1 \end{matrix} \middle| \sin^2 \phi \right) {}_2F_1 \left( \begin{matrix} -n, n+1 \\ 1 \end{matrix} \middle| \sin^2 \Phi \right). \quad (\text{B1})$$

The dependence on  $x$  and  $x'$  is generated by the product of the  ${}_2F_1(\cdot)$ , which is a symmetric bi-variate polynomial in  $x$  and  $x'$  of mixed order  $2n$ . The basic examples are

$${}_2F_1 \left( \begin{matrix} -n, n+1 \\ 1 \end{matrix} \middle| \sin^2 \phi \right) {}_2F_1 \left( \begin{matrix} -n, n+1 \\ 1 \end{matrix} \middle| \sin^2 \Phi \right) \\ = \begin{cases} 1 & n=0, \\ -1 + 2(x^2 + x'^2) & n=1, \\ 1 - 6(x^2 + x'^2 - x^4 - x'^4 - 4x^2x'^2) & n=2, \\ -1 + 12(x^2 + x'^2) - 30(x^4 + x'^4 + 4x^2x'^2) + 20(x^6 + x'^6 + 9x^4x'^2 + 9x^2x'^4) & n=3. \end{cases} \quad (\text{B2})$$

The simplicity of this format might be unexpected in view of the square roots in (41), but if (38) is constructed term-by-term on the right hand side by balancing the powers in  $k$  on both sides of the Neuman series, the linear coupling of  $k$  and  $x, x'$  in the arguments on the left hand side makes this plausible.

The piston contribution is manipulated by adding some  $\delta_n$  to these products, which by Mercer's theorem effects the piston's  $\lambda_{p,0}^2$ . To suppress the piston, equation (37) and the orthogonality of the  $K_p^{(0)}(x)$  suggest that

$$\int_{\epsilon}^1 x' dx' \int_{\epsilon}^1 x dx \left[ {}_2F_1 \left( \begin{matrix} -n, n+1 \\ 1 \end{matrix} \middle| \sin^2 \phi \right) {}_2F_1 \left( \begin{matrix} -n, n+1 \\ 1 \end{matrix} \middle| \sin^2 \Phi \right) + \delta_n \right] = 0. \quad (\text{B3})$$

Insertion of (B2) yields for example

$$\delta_n = \begin{cases} -1 & n=0, \\ -1 - 2\epsilon^2 & n=1, \\ -5(1 + 2\epsilon^2 + 2\epsilon^4) & n=2, \\ -31(1 + 2\epsilon^2) - 10\epsilon^4(8 + 7\epsilon^2) & n=3, \\ -229(1 + 2\epsilon^2) - 2\epsilon^4(334 + 329\epsilon^2 + 294\epsilon^4) & n=4, \\ -1891(1 + 2\epsilon^2) - 14\epsilon^4(403 + 488\epsilon^2 + 408\epsilon^4 + 396\epsilon^6) & n=5. \end{cases} \quad (\text{B4})$$

The first value removes the entire term at  $n = 0$  in (B1). The results in the main section added the  $\delta_n$  to all  $n \leq 10$ .

- 
- [1] Abramowitz, M., and I. A. Stegun (eds.), 1972, *Handbook of Mathematical Functions* (Dover Publications, New York), 9th edition, ISBN 0-486-61272-4.
- [2] Avila, R., A. Ziad, J. Borgnino, F. Martin, A. Agabi, and A. Tokovinin, 1997, *J. Opt. Soc. Am. A* **14**(11), 3070.
- [3] Bailey, W. N., 1929, *Proc. Cambr. Phil. Soc.* **25**(1), 48.
- [4] Béchet, C., M. Tallon, and E. Thiébaud, 2009, *J. Opt. Soc. Am. A* **26**(3), 497.
- [5] Boreman, G. D., and C. Dainty, 1996, *J. Opt. Soc. Am. A* **13**(3), 517.
- [6] Buscher, D. F., J. T. Armstrong, C. A. Hummel, A. Quirrenbach, D. Mozurkewich, K. J. Johnston, C. S. Denison, M. M. Colavita, and M. Shao, 1995, *Appl. Opt.* **34**(6), 1081.
- [7] Buser, R. G., 1971, *J. Opt. Soc. Am.* **61**(4), 488.
- [8] Chesnokov, S. S., and S. E. Skipetrov, 1997, *Opt. Commun* **141**(3-4), 113.
- [9] Clifford, S. F., 1971, *J. Opt. Soc. Am.* **61**(10), 1285.
- [10] Colavita, M. M., M. Shao, and D. H. Staelin, 1987, *Appl. Opt.* **26**(19), 4106.
- [11] Conan, R., 2000, *Modélisation des effets de l'échelle externe de cohérence spatiale du front d'onde pour l'observation à Haute Résolution Angulaire en Astronomie*, Ph.D. thesis, Université de Nice.
- [12] Conan, R., 2008, *J. Opt. Soc. Am. A* **25**(2), 526.
- [13] Conan, R., A. Ziad, J. Borgnino, F. Martin, and A. Tokovinin, 2000, in *Interferometry in Optical Astronomy*, edited by P. J. Lena and A. Quirrenbach (Int. Soc. Optical Engineering), volume 4006 of *Proc. SPIE*, pp. 963-973.
- [14] Coulman, C. E., and J. Vernin, 1991, *Appl. Opt.* **30**(1), 118.
- [15] Coulman, C. E., J. Vernin, Y. Coqueugniot, and J. L. Caccia, 1988, *Appl. Opt.* **27**(1), 155.
- [16] Dayton, D., B. Pierson, B. Spielbusch, and J. Gonglewski, 1992, *Opt. Lett.* **17**(24), 1737.
- [17] Ellerbroek, B. L., 1997, *Appl. Opt.* **36**(36), 9456.
- [18] Erdélyi, A., W. Magnus, F. Oberhettinger, and F. G. Tricomi (eds.), 1953, *Higher Transcendental Functions*, volume 2 (McGraw-Hill, New York, London).
- [19] Fried, D. L., 1977, *J. Opt. Soc. Am.* **67**(3), 370.
- [20] Fried, D. L., 1978, *J. Opt. Soc. Am.* **68**(12), 1651.
- [21] Fusco, T., N. Ageorges, G. Rousset, D. Rabaud, E. Gendron, D. Mouillet, F. Lacombe, G. Zins, J. Charton, C. Lidman, and N. Hubin, 2005, in *Advancements in Adaptive Optics*, edited by D. B. Calla, B. L. Ellerbroek, and R. Ragazzoni (Int. Soc. Optical Engineering), volume 5490 of *Proc. SPIE*, p. 118.
- [22] Fusco, T., G. Rousset, D. Rabaud, E. Gendron, D. Mouillet, F. Lacombe, G. Zins, P.-Y. Madec, A.-M. Lagrange, J. Charton, D. Rouan, N. Hubin, *et al.*, 2004, *J. Opt. A* **6**(6), 585.
- [23] Glindemann, A., 1994, *J. Opt. Soc. Am. A* **11**(4), 1370.
- [24] Goodman, J. W., 1985, *Statistical Optics* (Wiley).
- [25] Gottschalk, J. E., and E. N. Maslen, 1988, *J. Phys. A: Math. Gen.* **21**, 1983.
- [26] Gradstein, I., and I. Ryshik, 1981, *Summen-, Produkt- und Integraltafeln* (Harri Deutsch, Thun), 1st edition, ISBN 3-87144-350-6.
- [27] Lewis, A. R., and V. H. Rumsey, 1977, *J. Opt. Soc. Am.* **67**(2), 178.
- [28] Linfield, R. P., M. M. Colavita, and B. F. Lane, 2001, *Astrophys. J.* **554**(1), 505.
- [29] Lloyd-Hart, M., R. Dekany, D. Sandler, D. Wittman, R. Angel, and D. McCarthy, 1994, *J. Opt. Soc. Am. A* **11**(2), 846.
- [30] Malacara, D., J. M. Carpio-Valadéz, and J. J. Sánchez-Mondragón, 1990, *Optics Engineering* **29**(6), 672.
- [31] Mathar, R. J., 2007, arXiv:0705.1700 [astro-ph] .
- [32] Noll, R. J., 1976, *J. Opt. Soc. Am.* **66**(3), 207.
- [33] O'Meara, T. R., 1977, *J. Opt. Soc. Am.* **67**(3), 318.
- [34] Pearson, J. E., and S. Hansen, 1977, *J. Opt. Soc. Am.* **67**(3), 325.
- [35] Rainville, E. D., 1945, *Bull. Amer. Math. Soc.* **51**(10), 714.
- [36] Roddier, N., 1990, *Opt. Eng.* **29**(10), 1174.
- [37] Sasiela, R. J., and J. D. Shelton, 1993, *J. Opt. Soc. Am. A* **10**(4), 646.
- [38] Takato, N., and I. Yamaguchi, 1995, *J. Opt. Soc. Am. A* **12**(5), 958.
- [39] Voitsekhovich, V. V., 1995, *J. Opt. Soc. Am. A* **12**(6), 1346.
- [40] Walters, D. L., D. L. Favier, and J. R. Hines, 1979, *J. Opt. Soc. Am.* **69**(6), 828.
- [41] Winker, D. M., 1991, *J. Opt. Soc. Am. A* **8**(10), 1568, E: [37].